Tandem organic light-emitting diode with a molybdenum tri-oxide thin film interconnector layer*

Lu Fei-Ping(路飞平), Wang Qian(王 倩), and Zhou Xiang(周 翔)†

State Key Laboratory of Optoelectronic Materials and Technologies, Sun Yat-Sen University, Guangzhou 510275, *China*

(Received 24 September 2012; revised manuscript received 15 November 2012)

A 10-nm-thick molybdenum tri-oxide (MoO_3) thin film was used as the interconnector layer in tandem organic light-emitting devices (OLEDs). The tandem OLEDs with two identical emissive units consisting of N,N′-bis(naphthalen-1-yl)-N,N′-bis(phenyl)-benzidine (NPB) / tris(8-hydroxyquinoline) aluminum (Alq_3) exhibited current efficiency–current density characteristics superior to the conventional single-unit devices. At 20 mA/cm^2, the current efficiency of the tandem OLEDs using the interconnector layers of MoO_3 thin film was about 4.0 cd/A, which is about twice that of the corresponding conventional single-unit device (1.8 cd/A). The tandem OLED showed a higher power efficiency than the conventional single-unit device for luminance over 1200 cd/m^2. The experimental results demonstrated that a MoO_3 thin film with a proper thickness can be used as an effective interconnector layer in tandem OLEDs. Such an interconnector layer can be easily fabricated by simple thermal evaporation, greatly simplifying the device processing and fabrication processes required by previously reported interconnector layers. A possible explanation was proposed for the carrier generation of the MoO_3 interconnector layer.

Keywords: tandem organic light-emitting device, MoO_3 thin film, interconnector layer

PACS: 72.80.Le, 78.60.Fi, 85.60.Jb **DOI:** 10.1088/1674-1056/22/1/037202

1. Introduction

Organic light emitting diodes (OLEDs) have attracted a lot of research interest due to their wide applications for flat-panel displays and solid state lighting.[1–8] A long operating lifetime must be ensured before the mass-production of OLEDs for use in daily life. Tandem OLEDs having two or more electroluminescence (EL) units vertically stacked in series through interconnector layers can meet this requirement because of their advantages of enhanced current efficiency and luminance at low current densities, as well as their prolonged lifetime as compared to the conventional single-unit devices.[9–16] In a tandem OLED, the interconnector layer plays an important role, serving as the charge generation layer, and it is critical for the performance of tandem OLEDs. Upon the application of an applied voltage, the interconnector layer will generate electrons and holes. The generated electrons and holes will be injected into the neighboring electron- and hole-transporting layers (ETL and HTL) of the light-emitting units, and recombine with holes injected from the anode side or electrons injected from the cathode side for light emission.

Up to now, many interconnector layers have been used in tandem OLEDs. Usually the interconnector layers used in tandem OLEDs have a bilayer structure, which can be formed by a metal–metal (or metal oxide) bilayer,[17,18] an organic–metal (or metal oxide) bilayer,[9,11–15] an organic–organic bilayer,[3,19–22] a bulk heterojunction,[23] or a hybrid interconnector layer.[24] In the interconnector layer formed with an organic–metal oxide bilayer, transition metal oxides (TMOs) are widely incorporated neighboring the HTL of the neighboring EL unit due to their high work function and high optical transparency in the visible region for photon output. Examples include vanadium oxide (V_2O_5),[12] molybdenum trioxide (MoO_3),[13,14,25,26] and tungsten trioxide (WO_3).[15,27,28] While the organic layer adjacent to the ETL of another neighboring EL unit is commonly n-type doped by alkaline metals or metal compounds (Li, Cs, Ca, Cs_2CO_3).[3,13,26,27,29] It can be noted that the fabrication of these interconnector layers typically requires sputtering or co-evaporation processes, and delicate handling care is necessary, somewhat inevitably complicating the fabrication process. In addition, there will be a strong micro-cavity effect when using the metal interconnector layers. Therefore, it is very important to develop interconnector layers with high transmittance and simple processing.

MoO_3 thin film has high transmittance in the wavelength range from 400 nm to 800 nm.[13] In general, MoO_3 thin films are used along with an n-type ETL in tandem OLEDs as the interconnector layer. In this case, tandem OLEDs can have double current efficiency compared with the conventional single-unit devices. However, a device using only the MoO_3 thin film as the interconnector layer will not have double current efficiency compared with the conventional single-unit device.[14,25,26]

In this paper, we demonstrate an interconnector layer which consists of only 10 nm MoO_3. The current efficiency

*Project supported by the Doctoral Foundation of the Ministry of Education of China (Grant No. 20100171110025), the State Key Laboratory of Optoelectronic Materials and Technologies, China (Grant No. 2010-RC-3-1), and the Fundamental Research Funds for the Central Universities, China (Grant No. 09lgpy25).

†Corresponding author. E-mail: stszx@mail.sysu.edu.cn

© 2013 Chinese Physical Society and IOP Publishing Ltd

of a two-unit tandem OLED is enhanced in comparison to that of the conventional single-unit device. The tandem OLED has a higher power efficiency than the conventional single-unit device for luminance over 1200 cd/m^2. A possible explanation is proposed for the carrier generation of the MoO3 interconnector layer.

2. Experiment

Table 1 shows the structures of the OLEDs used in this study, all devices have an active area of 0.30 cm^2. All materials were commercially purchased and used as received. In tandem OLEDs, the two emissive units used were identical and consisted of N,N′-bis(naphthalen-1-yl)-N,N′-bis (phenyl)-be- nzidine (NPB)/tris(8-hydroxyquinoline) aluminum (Alq_3). All devices were fabricated on pre-cleaned and oxygen-plasma treated ITO-coated glass with sheet resistance of 10 Ω/□ and thickness of 80 nm. A thermally deposited Al film was used as the cathode. ITO substrates were ultrasonically cleaned in acetone, ethanol, and deionized water successively, then treated by O_2 plasma at the pressure of 42 Pa for 10 min. Finally, the treated ITO substrates were directly transferred, without exposure to air, into a vacuum chamber. All the films were thermally evaporated in an ultra high vacuum (UHV) growth chamber without breaking the vacuum. The organic, Al, MoO_3, and LiF thin films were thermally evaporated in the UHV growth chamber at base pressures of around 3–5 $\times 10^{-8}$ Torr, 2–6 $\times 10^{-6}$ Torr, 4–7 $\times 10^{-8}$ Torr, and 4–7 $\times 10^{-8}$ Torr, respectively. The evaporation rates were controlled with a quartz thickness monitor, and were 0.8 Å/s, 5 Å/s, 0.3 Å/s, and 0.3 Å/s for organic, Al, MoO_3, and LiF materials, respectively. The glass substrates were rotated during the deposition process by means of a rotary working holder at a speed of 12 rev/min so as to obtain uniform thickness thin films. The current density–forward direction luminance–voltage characteristics of the devices were measured using a Keithley SMU 236 source measure unit and a commercial luminance meter equipped with a calibrated silicon photodiode (ST-86LA, from the Photoelectric Instrument Factory of Beijing Normal University, China) at room temperature in air immediately after device fabrication. The EL spectra of the devices were recorded using a fiber spectrometer (Ocean Optics USB 2000), the capacitance–voltage (C–V) curves were measured with an Agilent 4284A LCR meter (Santa Clara, CA).

Table 1. Structures of devices, here EL represents NPB(40 nm)/Alq_3(80 nm).

Device	Structure
Device A	ITO/EL/LiF(2 nm)/Al(100 nm)
Device B	ITO/EL/EL/LiF(2 nm)/Al(100 nm)
Device C	ITO/ EL/MoO_3(10 nm)/EL/LiF(2 nm)/Al(100 nm)
Device D	ITO/LiF(100 nm)/Alq_3(80 nm)/NPB(40 nm)/LiF(2 nm)/Al(100 nm)
Device E	ITO/LiF(100 nm)/ Alq_3(80 nm)/MoO_3(10 nm)/NPB(40 nm)/LiF(100 nm)/Al(100 nm)
Device F	ITO/Alq_3(80 nm)/NPB(40 nm)/LiF(2 nm)/Al(100 nm)
Device G	ITO/Alq_3(80 nm)/MoO_3(10 nm)/NPB(40 nm)/LiF(2 nm)/Al(100 nm)

3. Results and discussion

Figures 1 and 2 show the current density–voltage (J–V) and the voltage–luminance (V–L) characteristics of devices A, B, and C. One can see that the driving voltage of device C is about twice that of the conventional single-unit device at the same luminance, but device B has an even higher driving voltage than device C. For example, at the luminance of 100 cd/m^2, the driving voltages are 3.1 V, 13.8 V, and 6.1 V for devices A, B, and C, respectively. This demonstrates that the 10 nm thick MoO_3 film used in device C can greatly improve both the J–V and the V–L characteristics of tandem OLEDs.

Figures 3 and 4 show the luminance versus current density and the current efficiency versus current density curves for devices A, B, and C, respectively. One can see from Figs. 3 and 4 that for a given current density, the luminance and the efficiency of device C are about twice of those of the conventional single-unit device. For example, at the current density of 20 mA/cm^2, the luminance reaches 780 cd/m^2 for device C, which is much higher than 416 cd/m^2 and 386 cd/m^2 for device B and the conventional single-unit device A. Also one can see that device B has a current efficiency similar to that of device A. The results show that upon the application of an

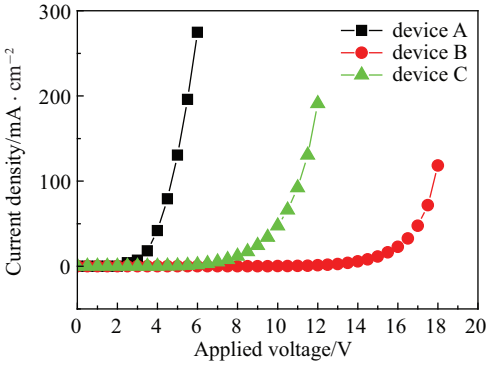


Fig. 1. (color online) The J–V characteristics of devices A, B, and C.

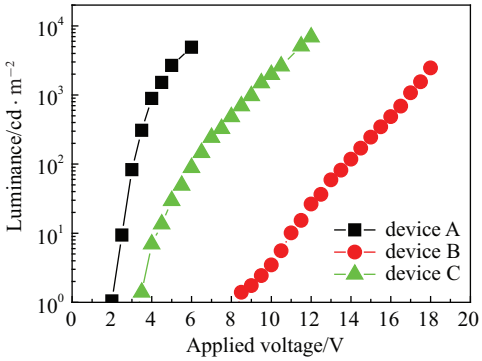


Fig. 2. (color online) The *L*–*V* characteristics of devices A, B, and C.

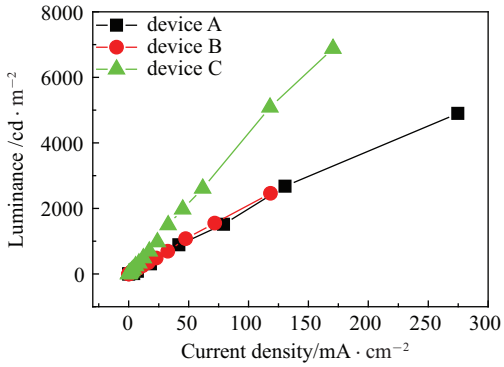


Fig. 3. (color online) The *L*–*J* characteristics of devices A, B, and C.

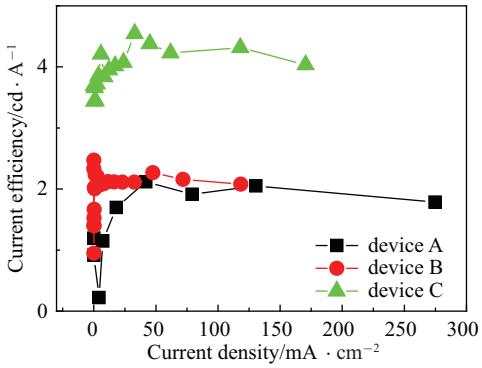


Fig. 4. (color online) Current efficiency–current density characteristics of devices A, B, and C.

applied voltage, the MoO_3 thin film between two emissive units will generate electrons and holes. The generated electrons and holes will be injected into the neighboring ETL and HTL of the individual EL unit, and recombine with holes injected from the anode side and electrons injected from the cathode side for light emission.

In general, the driving voltage will be multiplied as the number of the light emitting units in tandem OLEDs increases, so the tandem OLEDs have a power efficiency similar with that of the conventional single-unit devices. Researchers have done much work to improve the power efficiency of tandem OLEDs, such as inserting a very thin ReO_3 film into the p–n junction interconnector,[30] or using $CsCO_3$ and MoO_3 to modify the interface of the organic heterojunction interconnector layer.[31] Those methods can make the charge generate more easily, and then lower the driving voltage of the device, thereby improve the power efficiency of tandem OLEDs. One can see from Fig. 5 that when using the MoO_3 thin film as the interconnector layer, the tandem OLED possesses an even higher power efficiency than the conventional single-unit device when the device's luminance is over 1200 cd/m^2. This demonstrates that tandem OLEDs based on MoO_3 thin films have higher current efficiencies and power efficiencies than the conventional single-unit devices. In a typical OLED structure with a reflective metal electrode, direct outgoing emission beams will interfere with the beams reflected by the metal electrode. The constructive interference could result in a higher current or power efficiency.[32] Here, we attribute the improvement of the power efficiency to the constructive interference in the tandem OLED.

In order to demonstrate that the MoO_3 thin film can effectively generate charge carriers, we fabricated devices D and E. The 100 nm thickness LiF thin films inserted at the interface of anode and cathode were used to block carriers inject into organic layers. As shown in Fig. 6, no change in capacitance with the applied voltages from –20 V to 20 V in device D is found, indicating no charge generation in the Alq_3/NPB interface. However, the capacitance of device E gradually increases over 0 V. Since no charge can be injected into the device, it is deduced that the origin of the change in the capacitance of device E should be the generated charge when inserting the MoO_3 thin film layer into the two light-emitting units. Many reports have proved that the electric field-induced charge-generation process takes place at the interface between MoO_3 and NPB.[13,25,33] The electrons transfer from the highest occupied molecular orbital (HOMO) of the NPB to the conduction band of MoO_3. The electron transfer also occurs in a vacuum-deposited MoO_3 layer from various defect states to the conduction band via thermal activation. Then, the generated electrons and holes are injected into the neighboring ETL and HTL of the individual light-emitting unit and recombine with holes injected from the anode side or electrons injected from the cathode side for light emission.

Furthermore, we fabricated devices F and G and then compared them with device A. As we all know, because of the high injection barrier (holes injected from anode into the Alq_3 thin film layer and electrons injected into the NPB thin film layer) and the very low carrier mobility (holes transport in the Alq_3 thin film and electrons transport in the NPB thin film), device F has a very small current density under an applied voltage. However, when inserting a MoO_3 thin film into the interface of NPB/Alq_3, the current density can be greatly improved, as shown in Fig. 7. These results show that the MoO_3 thin film is essential to the charge generation and separation process in tandem OLEDs.

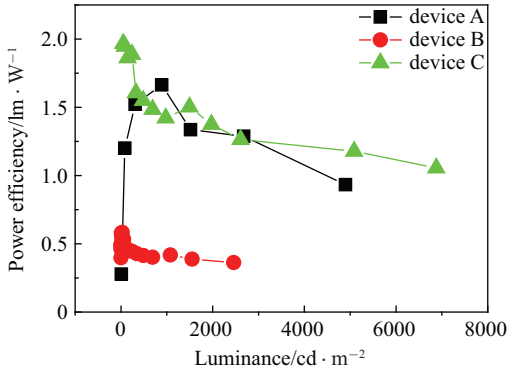


Fig. 5. (color online) Power efficiency–luminance characteristics of devices A, B, and C.

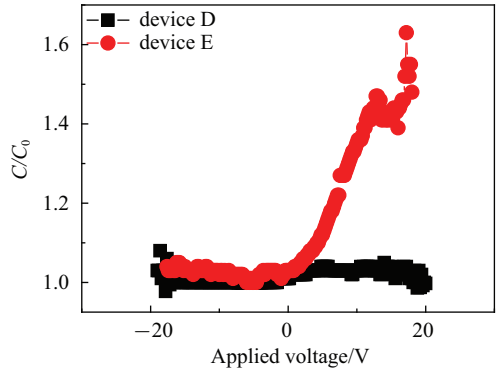


Fig. 6. (color online) The C–V characteristics of devices D and E.

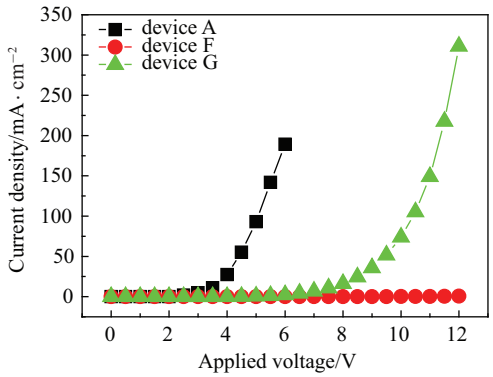


Fig. 7. (color online) The $J-V$ characteristics of devices A, F, and G.

Ultraviolet photoemission spectroscopy (UPS) analyses have shown the formation of an interface dipole upon the deposition of NPB on MoO_3. A p–n junction is formed between NPB and MoO_3 with a small hole injection barrier height.[25,33] It is expected that an electric-field-assisted charge generation and separation process can easily occur at the MoO_3/NPB interface via hole injection from MoO_3 into the HOMO of NPB. The charge generation process could also happen within the MoO_3 layer by exciting electrons from the oxygen vacancy derived gap states to the conduction band. In fact, similar results have been found at the interface between other transition metal oxide and the hole transport layers, such as vanadium oxide (V_2O_5)[12] and tungsten trioxide (WO_3).[15,27,28] In order to make the electrons inject into the light emitting unit easily, researchers always use the doping method to make the electron transport layer be n-type materials. On one hand, this method facilitates the generated electrons' injection into the ETL of the neighboring EL unit from MoO_3, on the other hand, it blocks the leakage of holes across the interconnector layer into the HTL of the other adjacent EL unit.[25,26,30] Here, we find that a tandem OLED based on only the MoO_3 thin film can achieve double current efficiency and an improved power efficiency compared with the conventional single-unit devices.

As mentioned above, holes and electrons can be injected from the anode and cathode into the organic layer, meanwhile they can be generated by the interconnector layers and then injected into a neighboring EL unit, as depicted in Fig. 8. For a tandem OLED, the charge balance factor can be defined as

$$\eta_1 = \frac{J_{h1} - J'_{h1}}{J} = \frac{J_{e1} - J'_{e1}}{J} = \frac{J_{r1}}{J}, \tag{1}$$

$$J_{r1} = \int_{x=0}^{L} eR_1(x)\,dx, \tag{2}$$

$$\eta_2 = \frac{J_{h2} - J'_{h2}}{J} = \frac{J_{e2} - J'_{e2}}{J} = \frac{J_{r2}}{J}, \tag{3}$$

$$J_{r2} = \int_{x=0}^{L} eR_2(x)\,dx, \tag{4}$$

where η_1 (η_2) is the charge balance factor, J_{h1} (J_{h2}), J'_{h1} (J'_{h2}), J_{e1} (J_{e2}), and J'_{e1} (J'_{e2}) are the injection and leakage current densities for holes and electrons in the EL unit 1 (2), respectively, as depicted in Fig. 8, L is the total thickness of an EL unit, $R_1(x)$ and $R_2(x)$ are the recombination coefficients for EL units 1 and 2, respectively, and e is the elementary charge. The recombination coefficient $R(x)$ can be expressed as

$$R(x) = \frac{4\pi q}{\varepsilon_0 \varepsilon_r}(\mu_n + \mu_p)(np - n_i), \tag{5}$$

where ε_0 is the permittivity of vacuum, ε_r is the relative dielectric constant of the organic materials, n, p, and n_i are the electron, hole, and intrinsic carrier concentrations, respectively, and μ_n and μ_p are the electron and hole mobilities, respectively.

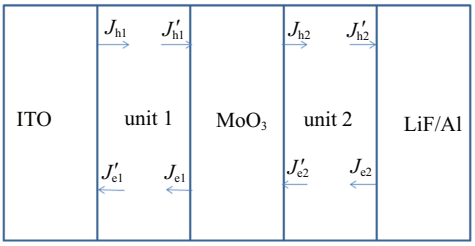


Fig. 8. Schematic diagram of the injection and leakage current densities for holes (J_h, J'_h) and electrons (J_e, J'_e) of both light emitting units.

The injection current densities J_{e1} and J_{h2} are comprised of two parts: the leakage current density from another EL unit and the current density generated by the interconnector layer. They can be expressed as

$$J_{e1} = J_{e0} + J'_{e2}, \tag{6}$$

$$J_{h2} = J_{h0} + J'_{h1}, \tag{7}$$

where J_{e0} and J_{h0} are the electron and hole current densities generated at the interface of MoO_3 and NPB, respectively. Under the steady state, we have

$$J_{e0} = J_{h0}. \tag{8}$$

From the principle of current continuality, the device current density J can be expressed as

$$J = J_{h1} + J'_{e1} = J_{e1} + J'_{h1} = J_{h2} + J'_{e2} = J_{e2} + J'_{h2}. \tag{9}$$

In general, the leakage current densities J'_{e1} and J'_{e2} are very small and can be ignored. From the above equations, if $J_{e2} \approx J_{e0}$, we can obtain $\eta_1 \approx \eta_2$. In this case, the tandem devices will have double current efficiency compared with the conventional single-unit devices. We attribute the double current efficiency of the tandem OLEDs prepared here to the similarity between the carrier injection abilities of the cathode and the interconnector layer.

4. Conclusion

In summary, tandem OLEDs with simple and effective interconnector layers, i.e., a 10-nm-thick MoO_3 thin film, have been demonstrated. It is demonstrated that tandem OLEDs exhibit superior current efficiency–current density characteristics compared to the conventional single-unit devices, and even have a higher power efficiency than the conventional single-unit devices. Furthermore, such an interconnector layer can be easily fabricated by simple thermal evaporation, greatly simplifying the device processing. The double current efficiency of the tandem OLEDs has been attributed to the similarity between the carrier injection abilities of the cathode and the interconnector layer.

References

[1] Reineke S, Lindner F, Schwartz G, Seidler N, Walzer K, Lussem B and Leo K 2009 *Nature* **459** 234
[2] Chen F P, Xu B, Zhao Z J, Tian W J, Lü P and Im C 2010 *Chin. Phys. B* **19** 037801
[3] Jiao Z Q, Wu X M, Hua Y L, Dong M S, Su Y J, Shen L Y and Yin S G 2011 *Chin. Phys. B* **20** 107803
[4] Meng L C, Lou Z D, Yang S Y, Hou Y B, Teng F, Liu X J and Li Y B 2012 *Chin. Phys. B* **21** 088504
[5] Yu J N, Zhang M Y, Li C, Shang Y Z, Lü Y F, Wei B and Huang W 2012 *Chin. Phys. B* **21** 083303
[6] Jiao Z Q, Wu X M, Hua Y L, Mu X, Bi W T, Bai J J and Yin S G 2012 *Chin. Phys. B* **21** 067202
[7] Suo F, Yu J S, Deng J, Jiang Y D, Wang R, Wang W Z and Liu T X 2007 *Acta Phys. Sin.* 56 6685 (in Chinese)
[8] Zhang X L, Yang S Y, Lou Z D and Hou Y B. 2007 *Acta Phys. Sin.* 56 1632 (in Chinese)
[9] Chiba T, Pu Y J, Miyazaki R, Nakayama K I, Sasabe H and Kido J 2011 *Org. Electron.* **12** 710
[10] Liao L S, Slusarek W K, Hatwar T K, Ricks M L and Comfort D L 2008 *Adv. Mater.* **20** 324
[11] Chen C W, Lu Y J, Wu C C, Wu E H E, Chu C W and Yang Y 2005 *Appl. Phys. Lett.* **87** 241121
[12] Tsutsui T and Terai M 2004 *Appl. Phys. Lett.* **84** 440
[13] Kanno H, Holmes R J, Sun Y, Cohen S K and Forrest S R 2006 *Adv. Mater.* **18** 339
[14] Chen P, Xue Q, Xie W F, Xie G H, Duan Y, Zhao Y, Liu S Y, Zhang L Y and Li B 2009 *Appl. Phys. Lett.* **95** 123307
[15] Chang C C, Hwang S W, Chen C H and Chen J F 2004 *Jpn. J. Appl. Phys.* **43** 6418
[16] Liao L S, Klubek K P and Tang C W 2004 *Appl. Phys. Lett.* **84** 167
[17] Zhang H M, Dai Y F, Ma D G and Zhang H M 2007 *Appl. Phys. Lett.* **91** 123504
[18] Sun J X, Zhu X L, Peng H J, Wong M and Kwok H S 2005 *Appl. Phys. Lett.* **87** 093504
[19] Fung M K, Lau K M, Lai S L, Law C W, Chan M Y, Lee C S and Lee S T 2008 *J. Appl. Phys.* **104** 034509
[20] Tang J X, Fung M K, Lee C S and Lee S T 2010 *J. Mater. Chem.* **20** 2539
[21] Cheng Y M, Lu H H, Jen T H and Chen S A 2011 *J. Phys. Chem. C* **115** 582
[22] Chen Y H, Tian H K, Chen J S, Geng Y H, Yan D H, Wang L X and Ma D G 2012 *J. Mater. Chem.* **22** 8492
[23] Chen Y H, Chen J S, Ma D G, Yan D H, Wang L X and Zhu F R 2011 *Appl. Phys. Lett.* **98** 243309
[24] Xiao J, Wang X X, Zhu H, Gao X , Yang Z H, Zhang X H and Wang S D 2012 *Appl. Phys. Lett.* **101** 013301
[25] Bao Q Y, Yang J P, Xiao Y and Deng Y H 2011 *J. Mater. Chem.* **21** 17476
[26] Hong K and Lee J L 2012 *J. Phys. Chem. C* **116** 6427
[27] Hamwi S, Meyer J, Kröger M, Winkler T, Witte M, Riedl T, Kahn A and Kowalsky W 2010 *Adv. Funct. Mater.* **20** 1762
[28] Meyer J, Kröger M, Hamwi S, Gnam F, Riedl T, Kowalsky W and Kahn A 2010 *App. Phys. Lett.* **96** 193302
[29] Cho T Yi, Lin C L and Wu C C 2006 *Appl. Phys. Lett.* **88** 111106
[30] Leem D S, Lee J H, Kim J J and Kang J W 2008 *Appl. Phys. Lett.* **93** 103304
[31] Chen Y H, Chen J S, Ma D G, Yan D H and Wang L X 2011 *Appl. Phys. Lett.* **99** 103304
[32] Lin C L, Cho T Y, Chang C H and Wu C C 2006 *Appl. Phys. Lett.* **88** 081114
[33] Yang J P, Xiao Y, Deng Y H, Duhm S, Ueno N, Lee S T, Li Y Q and Tang J X 2012 *Adv. Funct. Mater.* **22** 600